February 13, 2026

We wish to thank both reviewers for their helpful and constructive comments. The reviewers' comments and questions are addressed below.

Reviewer 2

In the manuscript "Estimating annual energy production of wake mixing control strategies including comparisons to wake steering," the authors quantify the impact on annual energy production (AEP) due to active wake mixing (AWM) and wake steering wind farm control strategies. A suite of high-fidelity large eddy simulations (LES) is used to fit an empirical Gaussian wake model. The empirical model is used to optimize and quantify the AEP gain of AWM and wake steering control at an offshore wind site in the New York Bight. The text is well written, and the methodology is clear. However, the model is not verified against out-of-sample data, raising concerns about the reported values for AEP gain. Furthermore, the influence of atmospheric conditions – specifically veer and turbulence intensity (TI), which has been highlighted in previous work to have a significant effect on the efficacy of flow control – is neglected in the modeling framework. Therefore, the degree to which the empirical model provides useful power predictions is uncertain, given that it is used almost ubiquitously to extrapolate across wind farm layouts, control strategies, and inflow conditions. Addressing these concerns would significantly strengthen the conclusions made in the manuscript.

Major Comments

1. The simulations from Frederik et al. WES (2025b) show that the optimal control strategy is sensitive to the ABL conditions, specifically wind veer and TI. This seems to undermine the central assumption that the relative power gains from AWM are not strongly sensitive to the wind conditions.

   We are not assuming that power gains from AWM are not strongly sensitive to wind conditions. We assume that AWM power gains: (1) depend strongly on wind direction and pitch amplitude; (2) are approximately invariant across Region II and early Region III wind speeds when turbulence intensity (TI) is low; and (3) diminish beyond a threshold wind speed and/or TI, where AWM is no longer beneficial. These first-order assumptions are guided by a prior AWM study as summarized in Table 2, where the non-zero entries indicate wind conditions where the power gains from AWM have been evaluated (or estimated) and found to be significant enough to justify its use. Higher in Region III, the utility of AWM is certain to diminish due to the lower wake effects. Similarly, AWM is expected to decrease at higher TI because increased ambient mixing reduces the benefit of externally-imposed mixing. Due to the computational expense of the LES, we therefore focused our training data on varying pitch amplitude and wind direction while simulating a single Region II wind speed and low TI level, and we built into the optimization algorithm a switch to disable AWM for wind speeds above 15 m/s or TI above 10%. In the original manuscript these assumptions and the training-data selection were split across Sections II and III, potentially confusing the reader. We have consolidated them so readers can clearly see what assumptions were made in the model.

   Additionally, the reviewer is correct that veer can have a large impact on the performance of different AWM models, particularly by skewing wakes downstream. The empirical Gaussian

model in FLORIS assumes an axisymmetric wake profile, and therefore cannot currently represent wake skewness due to veer. As a result, our AEP analysis is limited to wind speed, wind direction, and turbulence intensity (TI) distributions from the NY Bight. The built-in FLORIS AEP tools are also designed around these wind speed/direction/TI inputs and do not include veer; however, we note in the conclusions that incorporating veer and shear effects is an important topic for future work.

2. The empirical Gaussian model is only evaluated on its calibration data. With many free parameters, it is unsurprising that the empirical model performs well in-sample. However, the same model is used to extrapolate to different wind directions (e.g., partial waking), turbine spacings (including 3D, where complexity in the near-wake may be significant), wind shear and veer, TI, pulse amplitudes beyond 4 degrees, and cases of wake steering. The results all rely on accurate model extrapolation, but there is no evidence that the model does well out-of-sample. Additional testing cases for model verification are necessary for the results in Section 4 to be trustworthy. Some related questions/comments:

   The reviewer is correct that uncertainty is a major factor in the results due to the limited training data. We trained the model using the full set of LES cases rather than reserving a subset for testing, given the high computational expense of LES and the limited number of simulations available. We agree that additional simulations and a dedicated testing set would be valuable for more robust uncertainty quantification and model refinements, and we view that as an important direction for future work. The focus of the present manuscript is on establishing a practical framework for estimating AEP gains due to AWM from a limited set of high-fidelity training data. We have mentioned this in the updated manuscript. Moreover, the authors no longer have access to the computational resources required to run additional LES cases. However, we have take further steps to acknowledge the uncertainty in the AEP results including: (1) clarifying in both the title and manuscript that this work is an AEP estimation strategy/framework based on engineering wake models, and not necessarily a definitive AEP estimate; (2) changing all results to report only AEP gains relative to the baseline FLORIS model (rather than absolute AEP values), so the focus is primarily on the additional AWM term in the empirical Gaussian model; and (3) pointing to recent advancements in uncertainty quantification (e.g., Aerts et al. [2025]) that could be leveraged in future studies to bound AEP estimates from low-fidelity, engineering-type models like FLORIS. Additional comments regarding uncertainty and the training data used in this study are provided below.

   - Are the helix and subharmonic pulse (St=0.15) cases used in model calibration?

     No, Line 272 as been updated to clarify that only the baseline LES cases and LES cases of the pulse method at $St = 0.3$ were used for tuning the FLORIS model. The update text is included below:

     "All of the baseline LES cases and the LES cases of the pulse method at $St = 0.3$ were used for tuning the FLORIS parameters. This includes the four baseline LES cases, which were used in the first step of the calibration, and the five AWM LES cases of the pulse method at $St = 0.3$, which were used in the second step of the calibration."

   - How is the parameter gamma tuned with only one value of freestream TI in all of the LES data?

     The linear dependence of TI in the mixing model is part of the standard empirical Gaussian model in FLORIS. The proportionality constant, γ, is calibrated here based

on the fixed TI level from the precursor using in the LES data. Thus extrapolating to other TI levels does introduce a large degree of uncertainty, which we have emphasized in the text. The focus of the results are on power gains normalized by the baseline wake, and we have not included a TI dependence in the AWM term – instead we assume that power gains over the baseline are relatively constant for low TI levels with Region II wind speeds, and turn off AWM for higher TI levels.

- There appear to be significant spatial differences between wakes modeled in FLORIS and LES (Figure 10). This causes concerns regarding model extrapolation.

  The wake profile comparisons in Figures 10 and 11 and the surrounding discussion were not intended to serve as a validation between FLORIS and the LES, but instead to highlight where the current emperical Gaussian wake model lacks degrees of freedom needed to represent flow features from the LES. The primary validation metric in this paper is Table 5, which indicates that FLORIS can provide a reasonable estimate of total farm power despite pointwise inaccuracies in the predicted flow fields (in part because farm power is an aggregate quantity that benefits from averaging across turbines). More generally, we do not expect FLORIS to match the LES wake profiles because it does not explicitly account for veer, shear, non-axisymmetric wake structure, induction effects, or strict conservation properties. As a result, agreement in farm power can occur even when the detailed flow fields differ. We have reworded this section in the updated manuscript to more clearly state the intention of these comparisons to the reader and to motivate future improvements to FLORIS and related reduced-order models, such as the skewed wake correction model of Abkar et al., Energies (2018) mentioned by the second reviewer.

3. In Figure 4, the variation in power production across the columns of the identically controlled turbines can be quite significant within each control configuration. For example, in the bottom left subfigure (Pulse, A=2 degrees, St=0.3, 6D spacing at 225 degrees), the power gain/loss changes sign in the third row across the columns. Are these physical, or a product of the short averaging time (600 sec)? How does this variation affect the wake model calibration and subsequent results presented in Section 4?

   The row-to-row and column-to-column variation seen in Figure 4 is likely dominated by statistical variability associated with the finite averaging window (600 s). It may also be due to physical farm-level effects (e.g., large-scale flow redistribution/blockage or lateral wake meandering) that can produce non-identical inflow conditions across columns even under identical turbine control. However, we did not explicitly study such effects here. We have mentioned both of these explinations in the update manuscript. For the wake-model calibration and the Section 4 results, this variability is partly mitigated because the FLORIS cases corresponding to these LES simulations are based on column-averaged wake behavior, which introduces an additional averaging step and reduces sensitivity to column-wise fluctuations. Consequently, the calibration is intended to capture the mean farm response rather than column-specific deviations.

4. Line 221, Equation 3: What is C? Is it constant or a function of streamwise position? Does the empirical Gaussian model conserve mass and momentum?

   We have updated the equations to better reflect the model details from the FLORIS documentation. The equations and surrounding description now read:

$$u/U_\infty(x,y,z) = 1 - C\exp\left(-\frac{(y-\delta_y(x))^2}{2\sigma_y(x)^2} - \frac{(z-\delta_z(x))^2}{2\sigma_z(x)^2}\right), \tag{1}$$

$$\sigma_{y,z}(x) = \int_0^x \sum_{i=0}^{n} k_i \mathbf{1}_{[b_i,b_{i+1}]}(x')dx' + M_j(x)dx' + \sigma_{y_0,z_0}, \tag{2}$$

$$M_j(x) = \omega_v \sqrt{\left[\sum_{\substack{i=1\\ i\neq j}}^{N_{turb}} \left(\frac{\Omega_{ij}a_i}{((x_j-x_i)/D_i)^2}\right)^2 + \left(\frac{A_j^p}{d}\right)^2 + (\gamma I)^2\right]} \tag{3}$$

$$C = \frac{1}{8\sigma_{0_D}^2}\left(1 - \sqrt{1 - \frac{\sigma_{y_0}\sigma_{z_0}C_T}{\sigma_y\sigma_z}}\right), \tag{4}$$

where j ranges from 1 to the total number of turbines, N_{turb}. There are several relevant parameters in Eqs. 1-3 for this study, which are described herein. The model for the velocity deficit in Eq. 1 depends on a scaling factor, C, which is given by Eq. 4, and wake widths σ_y and σ_z, which are given by Eq. 2. The wake widths are specified by a constant initial wake width, σ_{y_0,z_0}, and a set of parameters, k_i, that control the wake expansion rate between break-point locations b_i and b_{i+1}. The initial wake widths are determined by an initial wake width parameter σ_{0_D} as $\sigma_{y_0} = \sigma_{0_D}R\cos(\phi)$ and $\sigma_{z_0} = \sigma_{0_D}R\cos(\tau)$ where R is the rotor diameter of the turbine and ϕ and τ are the yaw and tilt angles, respectively. The user-manual recommends default values for the initial wake width parameter, σ_{0_D}, that should be satisfactory for most applications, and anticipates that no more than 3 expansion rates (along with 2 break points) should be needed to describe the wake expansion ($n = 2$ in Eq. 2). These guidelines are followed here.

Lastly, no, there is no notion of conservation of mass or momentum in the empirical Gaussian model.

- Additionally, is Equation 3 a function of x only, or of (x, y, z)? The velocity is a function of x,y,z. This is updated in the equations listed above.
- What effect would including the skewed wake correction (Abkar et al., Energies (2018)) in the Gaussian wake model have on the model results?

  A skewed wake correction may allow the FLORIS model to better capture the effects of veer, which primarily skews the LES wakes, although such corrections are not considered here.

5. Figure 12: The drop in power (or energy production? Please clarify) between all wind conditions and conditions where at least one turbine is actuated is nearly one order of magnitude. However, in the tightest spacings, at least one turbine is actuated upwards of 30% of the time (Figure 13, left). Showing dimensional energy generation binned by operating condition could help explain this further (e.g., amount of energy generation for conditions favoring AWM and without AWM).

   Figure 12 is depicting baseline-normalized power averaged over a set of wind conditions. The reviewer is correct that this needs clarification because the symbol P was used to represent both instantaneous power at a wind condition (in equation 11) and averaged power in Figure

12. We have updated the figure and caption so it is clear we are using average power, denoted $\bar{P}$.

Moreover, the reviewer points out an interesting finding, which is that AWM is often used in tighter configurations at off-angle wind directions even while there is not an extraordinary influence on the energy generation for these cases. One of the findings of this work is that the possible improvements with AWM may be relatively small for the case studied, and this may be a function of the operating range of AWM being skewed towards lower wind speeds that have less energy available (since power scales with velocity cubed). We have noted this in the updated manuscript. The reviewer's suggestion of binning on dimensional energy generation versus operating condition is thus well received, although we have elected not to include it in the manuscript for the sake of brevity.

- Related: In Figure 14, right, it is surprising that the orientation of the wind farm has a relatively small impact on the normalized AEP gain, given how sensitive the benefits to AWM are to the wind direction (shown in Figure 12). Yet the difference between the "worst-case" and "best-case" wind farm orientation only changes the AEP gain by order 0.05%. It may be useful to see how the power gain due to AWM changes with wind direction averaging sector, for example at fixed pulse amplitude

Although the AWM benefit is strongly wind-direction dependent when conditioning on a fixed inflow (as shown in Figure 12), the normalized AEP gain in Figure 14 is computed after averaging over the full wind-rose and wind speed/TI distributions, including periods when AWM is disabled (high wind speed/high TI) and periods with only partial waking (see comment 7). This averaging substantially reduces sensitivity to farm orientation, although the remaining peak gain still occurs near alignment with the dominant direction in the site distribution. The authors agree that the AEP AWM results are not particularly sensitive to the angle of orientation of the wind farm, and this returns to the point in the previous comment that the operating range of AWM is skewed towards lower wind speeds that have less energy available, so the dimensional change in power with AWM is muted.

6. It may help to show a PDF of power gains due to AWM as a function of turbine spacing distance to explain the non-monotonicity in Figure 12 (conditioned on > 0 AWM turbines). The hypothesis stated in the text is that AWM is used more selectively as spacing increases, but that does not necessarily translate to higher power gains when AWM is used.

The non-monotonicity in the fourth panel of Figure 12 in the original manuscript is explained by Figures 1, 2, and 3 in this document. Specifically, Figure 1 shows the baseline-normalized farm power over wind conditions where at least one turbine is actuated to maximize farm power (i.e., AWM is being used), and where the wind direction is within 5°, 15°, and 25° of the wind farm orientation angle, 225°. For a 5° offset in wind direction, the trend is monotonic, with greater average power gains observed for tighter spaced farms. However, as the wind direction offset increases to 25°, the trend flips, with larger average power gains occurring for the $6D$-$8D$ spaced farms. Moreover, notice that the baseline-normalized power is relatively constant for the larger spaced farms across all panels in Figure 1, but decreases for the smaller spaced farms. This trend is explained by the results in Figure 2, which have been updated from the original manuscript to show the usage of wake mixing (and wake steering) binned on wind direction at 1° increments. For the wind farms with a diagonal

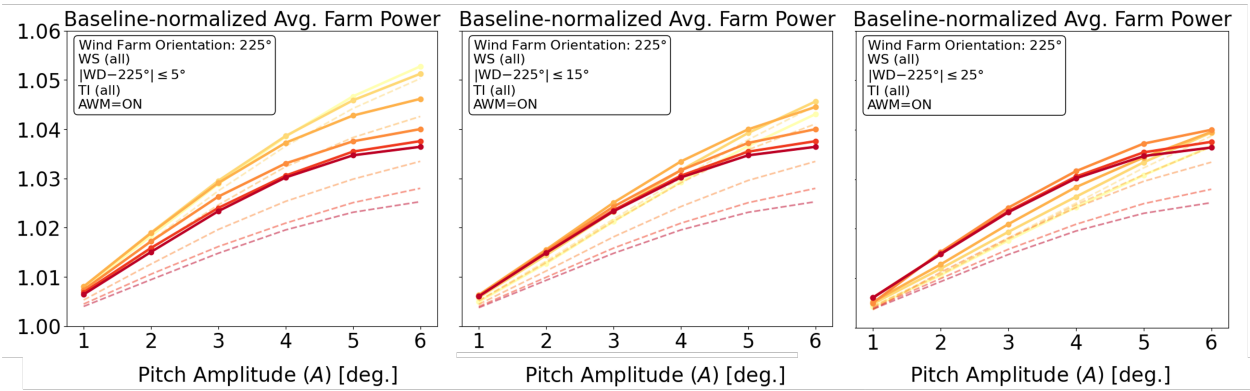

Figure 1: Baseline-normalized total average farm power of the AWM pitch amplitude. The wind farm is oriented at 225° and the turbine spacing is varied from $3D$ to $8D$ as the colors go from light to dark. Each panel averaged over wind conditions where at least one turbine is actuated to maximize farm power, and where the wind direction is within 5° (left), 15° center, and 25° (right) of 225°. The cases where $N_{AWM} = 9$ and $N_{AWM} = 3$ are shown by solid and dashed lines, respectively.

spacing of $6D$-$8D$ between turbines, AWM is only used at 90° and 45° angles relative to the wind farm orientation – this is where direct geometric alignment between three turbine columns occurs. However, for the smaller spaced farms, AWM is also used at an additional intermediate angle at 22.5° increments. At these angles two turbines wake a downstream turbine and it is beneficial to apply wake mixing. For the wind farms with a larger footprint, however, the separation distance between turbines at these angles is large enough that no significant waking occurs and so AWM is not applied. Consequently, these conditions are not included in the power results in Figure 1 for the larger spaced farms. Hub-height planes showing streamwise velocity from two example wind farms with an incoming wind direction of 250° are shown in Figure 3 to demonstrate this behavior. At these intermediate angles, there is a lower baseline-normalized power gain than at 45° or 90°, where 3 turbines wake two rows of downstream turbines. Thus, on average, there is a larger gain in power for the $6D$-$8D$ spaced wind farms when AWM is being used than the $3D$-$5D$ spaced farms. This is the sense in which we originally stated that AWM was being used more selectively for the larger spaced farms. We have clarified this language in the updated manuscript along with the updated version of Figure 2. We thank the reviewer for encouraging us to fully explore this result. Lastly, note this trend is only true when $N_{AWM} = 9$; for $N_{AWM} = 3$, the power gains for the smaller spaced farm still outperform the larger spaced farms, indicating significant gains from mid farm actuation.

7. Previous work has observed the greatest power gain due to wake steering in partial waking, rather than in the fully-waked case (e.g., Tamaro et al. WES 2025). This is not observed in the proposed model (Line 410). If only partial wake conditions are considered, is this observed in the present model as well?

   Yes, if we limit the wind direction to only include partially wake conditions, wake steering generally outperforms wake mixing (see Figure 4 in this document) and the gains outperform those observed with wake steering when fully-waked wind-directions are included. This is

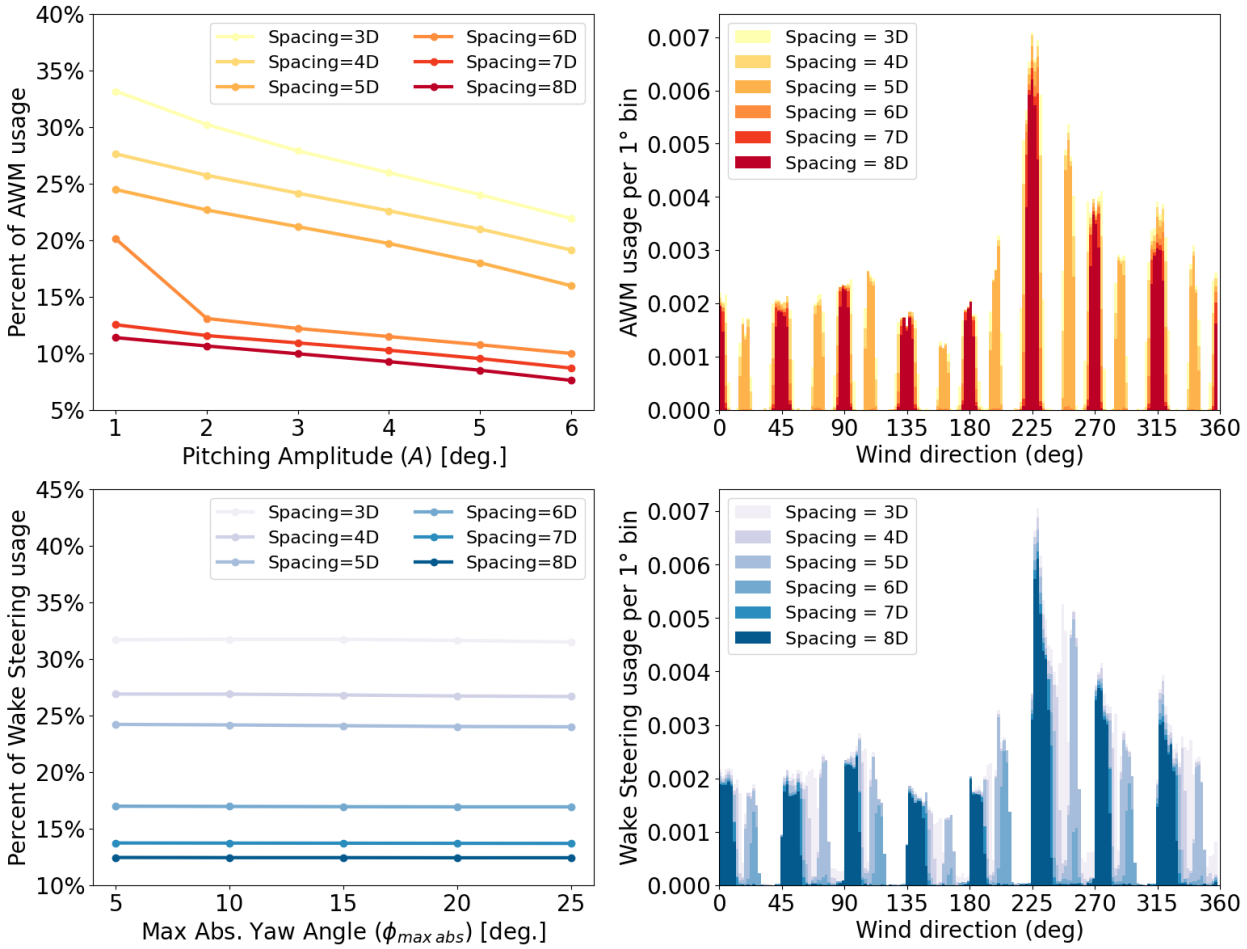

Figure 2: The usage of wake mixing (top) and wake steering (bottom) across all wind conditions in the Weibull distribution. The left panels show the total percent of wind conditions where the optimization routine actuated/yawed at least one turbine in the wind farm in order to maximize farm power. In the right panels, the usage of each control strategy is shown binned on wind direction for the case where $A = 4°$ and $\phi_{max\ abs} = 10°$. For the data presented here, the wind farm is oriented at 225° and the turbine spacing is varied from $3D$ to $8D$.

mentioned in the updated manuscript. Moreover, the updated wake mixing and wake steering usage results shown in Figure 2 clearly indicate that wake steering is used more often in partially wake scenarios.

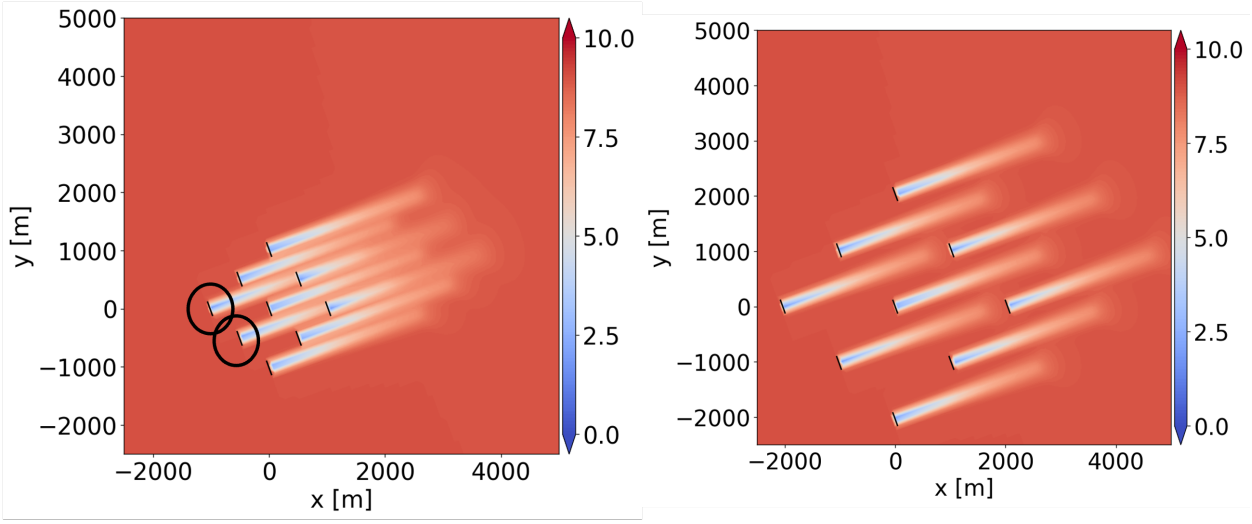

Figure 3: Hub height planes showing streamwise velocity of the wind farms with $4D$ (left) and $6D$ (right) diagonal spacing between turbines. The incoming wind direction is 250°. In the right panel, two frontline turbines are actuated to maximize total farm power as indicated by the black circles. In the left panel, all turbine are operating with baseline controls – there is no benefit to using AWM in this case because of the large separation between turbines along the direction of the incoming wind.

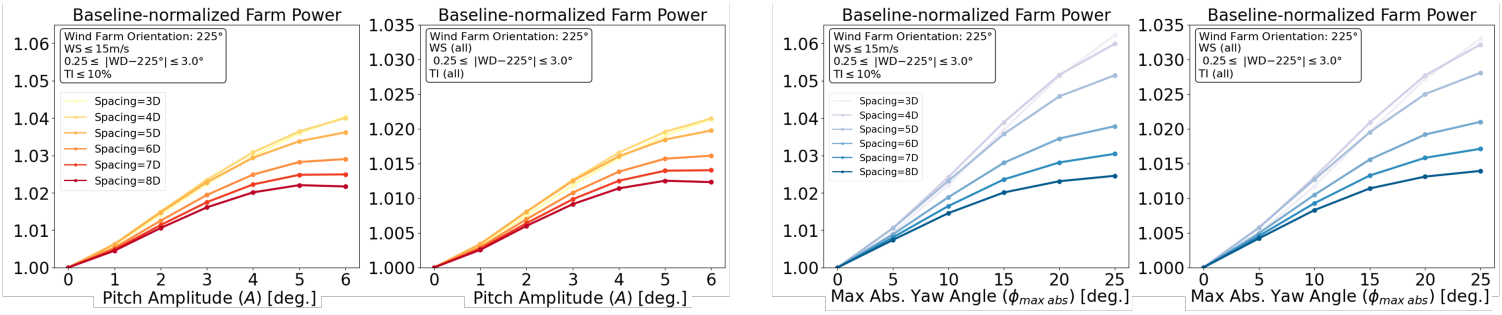

Figure 4: Baseline-normalized farm power in partial waked conditions for both AWM and wake steering. In each panel, the wind direction, WD, is limited to $0.25° \leq |WD - 225°| \leq 3°$, and the wind speed and TI ranges are adjust to include conditions where $WS \leq 15$ m/s and $TI \leq 10\%$, as well as all wind speed and TI in the Weibull.

Minor Comments

- Line 040: 1 sentence regarding why previous reduced-order models were not used in this work would be useful.

  We have clarified that the referenced models are mid-fidelity models, unlike FLORIS which is a low-fidelity engineering model designed for rapid wind farm layout and control optimization.

- Line 055 (and more generally): Why is AWM vs wake steering presented as an either/or decision? The general narrative of the paper leans toward "choosing between" wake steering and AWM, rather than the possible synergy between the two strategies. Parts of the introduction,

results (specifically Section 4.2), and conclusions could be reworked to provide a more synergistic perspective on flow control strategies for wind farm operation.

The manuscript is aimed at comparing AWM to wake steering, although combined control methods that harness the benefit of both control strategies are of interest to the authors and will be considered in future work. With the current capabilities of FLORIS, optimizing wake steering and wake mixing is (perhaps surprisingly) very distinct tasks and writing a joint optimization routine would take significant work. We have included this as an area of future work in the conclusion.

- Line 082: It would be useful to give an estimation of grid cell size in the rotor region and between turbines. Related, is it necessary to simulate with such high resolution? 1 billion grid cells is a massive computational expense.

  The grid cell size is shown in Figure 2 of the manuscript. A resolution of 2.5 m is used in the rotor region of the turbine and between turbines in the wind farm. A background resolution of 5 m is used outside of the wind farm. We have found that a resolution of 2.5 m in the rotor region is necessary for accurately calibrating the actuator line model of the IEA 15MW to the power curve, and we opted to maintain this resolution between turbines to avoid numerical issues that arise when resolved turbulence convects through coarsening/refining grids.

- Line 090: Please give a rate of surface cooling and roughness for reproducibility. ABL profiles (perhaps in an appendix or reference to other work) would be useful as well. Are these the exact same LES cases as Brown et al. (2025)?

  This sentence has been updated to include the surface cooling rate and roughness:

  "Specifically, a negative ground temperature rate of -0.12 K/hr and a non-zero surface roughness of 0.0005 m were introduced in the precursor simulations to closely match mean hub-height and rotor-averaged statistics of the Med. WS/Low TI case."

  These are indeed the same values from Brown et al. (2025).

- Figure 2, right subfigure: It seems like the turbine numbers (or wind direction) are mislabeled, as the 206.5 degree wind direction should lie between the 180 and 225 degree wind directions. Visually, the plot appears to show more like 160 degrees orientation. Defining the heading angle may help to clarify this.

  The caption of Figure 2 has been updated with the following sentence to clarify the heading:

  "The panels show the 3×3 wind farm oriented at 225°, 180°, and 206.5°, with 0° defined as north/up and bearing measured clockwise, following wind-rose convention."

- Figure 3: The important turbine parameters for this study (rated wind speed and dimensions) can simply be put in-text and this figure can be omitted.

  The authors want to leave this figure in place as it gives an accessible means to recall the power curve of the IEA-15 MW, and the power curve is important in the assumed operating ranges of AWM.

- Table 3: It is an interesting result that using the pulse method, the 5D spacing with AWM is approximately equal to the 6D spacing with baseline control. This is a saving in footprint area of 30% for the same power output. Perhaps this could be explored further in the text.

The authors agree that arguments surrounding the increased power density potential of AWM (and wake steering) are under-reported in literature. Indeed, they are under-reported in our manuscript, as well! Although we are not aware of a consensus means to estimate the value of saving space versus AEP gains, we have added a note in the manuscript to the highlight the reviewer's point. Thank you.

- Figure 4: The black text on the darkest red squares is difficult to read (consider switching these squares to white text, or outlining the text in white)

  Thank you for the suggestion. We have opted to keep the current formatting after some experimentation for consistency and to avoid appearing to be highlighting any specific turbines in the figure.

- Line 189: How are rotor-averaged velocities computed as a function of streamwise position? Possibly related – Figure 5, top right subfigure: Why is the freestream quantity $u/u_{baseline}$ approximately 0.33 (and not 1, for example)?

  We have clarified in the caption of Figure 5 in the manuscript that rotor-averaged velocities are computed by averaging the streamwise velocity over the rotor-disc area. Moreover, there was indeed a 1/3-factor missing in the right subfigure. The updated results are shown in Fig. 5. Thank you very much for noticing this mistake.

- Line 192: Is the higher rotor-averaged velocities behind the third row turbine between the St=0.3 and subharmonic St=0.15 pulse turbines due to wake physics (mixing), or due to the fact that the third row turbine in the subharmonic AWM strategy extracts more power (and imparts a higher thrust)?

  Both factors may be contributing. The turbulent entrainment results shown in Figure 6 of the original manuscript do indicate some additional entrainment behind the third row of turbine at $St = 0.3$ when compared to $St = 0.15$, and the reviewer is correct that the third row of turbines extract more power for the subharmonic case.

- Figure 6: What are the colorbar units? Also, the contours show regions of elevated turbulent entrainment behind the first row, but decreased turbulence entrainment further downstream. I would anticipate that this would have detrimental effects downstream if the wind farm extended beyond the third row of turbines.

  The units of the mean turbulent transport terms are simply velocity cubed (mean velocity times Reynolds stress). It would indeed be interesting to study the effects of AWM beyond the third row of turbines, and even potential mid-farm actuation. The rotor-averaged velocities shown in Figure 5 of this document suggest there would still be some benefit for a fourth row of turbines for all of the pulse control strategies.

- Figure 7: Differences between subplots are difficult to discern as plotted. Consider showing the difference in u between the baseline case, or remove this figure.

  We have updated this plot to show baseline subtracted streamwise velocities. See Figure 6 in this document.

- Figure 8: Demarcating the position of the downstream turbine in the right four subfigures would clarify elements of this figure.

  We have added arrows to demarcate the two turbines in the right four subfigures (see Figure 7).

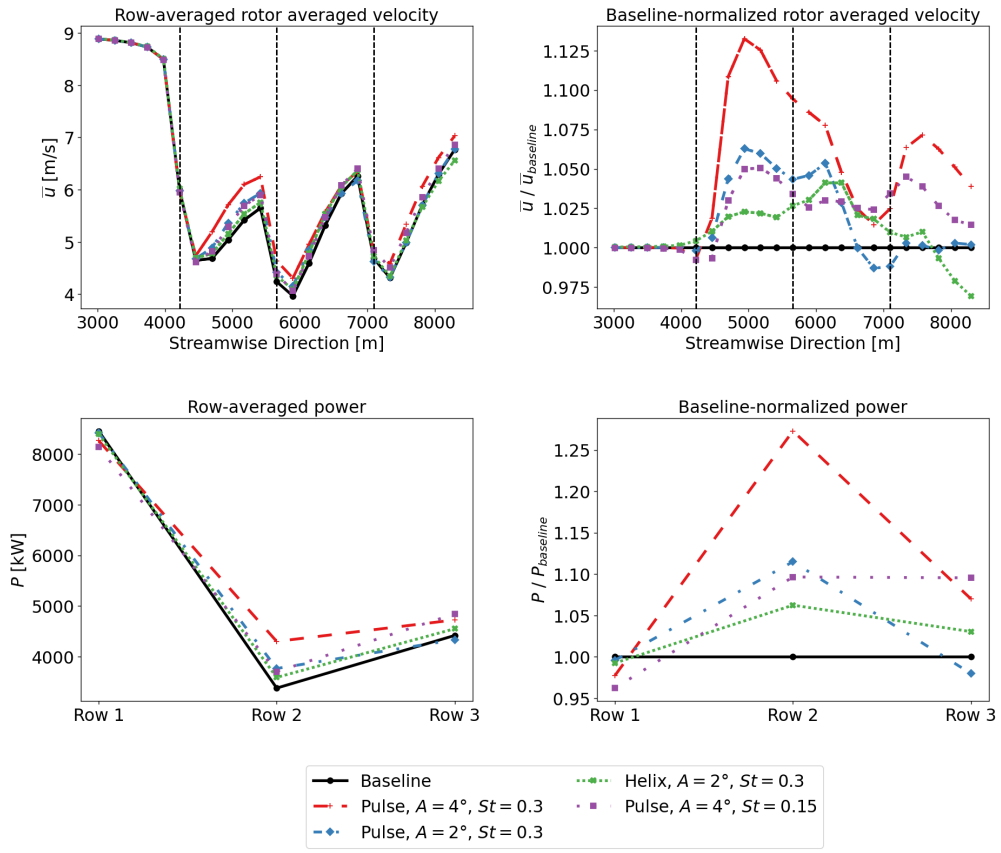

Figure 5: Row-averaged rotor-averaged velocity and power. Both the absolute and baseline-normalized values are shown. Included are results from the $6D$-spaced wind farms oriented with the wind direction at 225°. Rotor-averaged velocities are computed by averaging the streamwise velocity over the rotor-disc area.

- Table 4: Please include all default values for variables in Equations 3-5 here (e.g., σ_{y_0}).

  Thank you, we have updated Table 4 to include the rotor-normalized initial wake width factor σ_{0_D}.

- Line 253: Can the W_fact parameter be interpreted simply as an adjustment to C_P?

  Yes, we have updated this line to indicate that the scaling factor W_{fact} corresponds to an adjustment of the FLORIS power coefficients, C_p.

- Figure 13, right: This subfigure seems out of place. Consider omitting altogether and move the main findings to the text (percent of conditions with yaw actuation is invariant of the maximum yaw angle and increases with increased spacing).

  This figure as been updated in reference to major comment number 6 to quantify wake mixing/steering usage binned on wind direction angles at 1° increments (see Figure 2 in this document and the surrounding discussion). We have also taken the reviewer's suggestion of clarifying in the text that the percent of wind conditions with yaw actuation is invariant of the maximum yaw angle and increases with increased spacing.

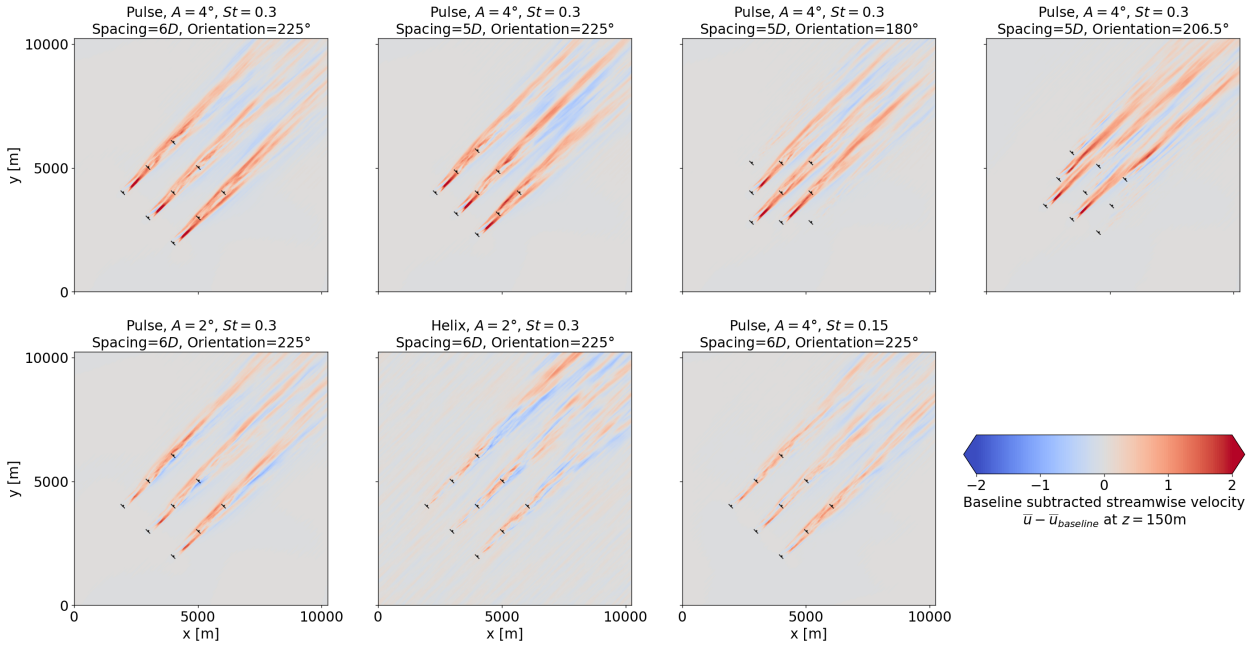

Figure 6: Baseline subtracted streamwise velocity contours on the hub-height plane at $z = 150$ m.

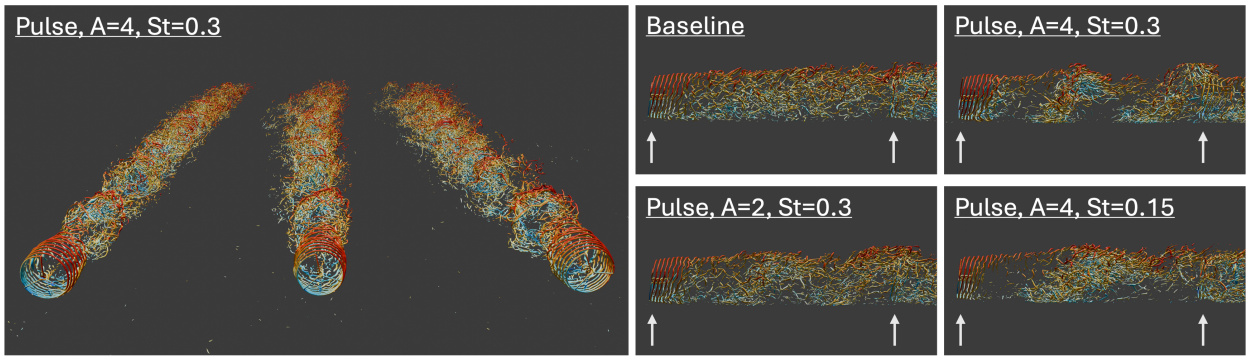

Figure 7: Flow visualization showing isosurfaces of the Q-criterion at $Q = 0.05$, colored by streamwise velocity. (Left) Isosurfaces of the $6D$-spaced wind farm, oriented with the wind direction at 225°, with pulse actuation at $A = 4°$ and $St = 0.3$. (Right) Wake profiles behind the actuated turbines for the baseline case and three different implementations of the pulse method. The arrows indicate the positions of the upstream and downstream turbines.

- Figure 16: Again, it is difficult to discern differences between contour plots. Consider showing differences in u between baseline and different control methodologies, or omit this figure.

  We have taken the reviewer's suggestion and removed this figure from the manuscript.

- Line 404: Please include the cosine-loss exponent values for thrust and power used in FLORIS.

  Thank you for this suggestion. We have updated this sentence to read:

  "In FLORIS, yaw misalignment is handled by the "cosine-loss" operational model, which reduces the nominal turbine power by a cosine-based correction. For the IEA 15 MW turbine,

we retain the default cosine-loss exponent of 1.88."

- Line 419: The comparison between "at least one actuated AWM turbine" and "at least one wake steering turbine" is not apples-to-apples because the amount of wake steering is not a binary variable. This should be highlighted in the text. (also in Line 445)

  We have clarified this sentence to indicate that the use of wake steering is quantified in this study by a non-zero value of $\phi_{max\ abs}$.

- Line 446: The full range of AEP gain due to wake steering (approximately 0.2% to 1.2%) is not reported in the conclusions, while the full range of AEP gain due to AWM is reported (0.1% to 0.4%), which is misleading.

  We've included the full range of AEP gains in the conclusion for both wake mixing and wake steering.

Technical Comments

- Line 069: Section 2.4 is not addressed in this paragraph.
  Thank you for noticing this omission. We have updated this paragraph to include Section 2.4.
- Line 092: How are the "rotor averaged shear" and "rotor-averaged veer" computed?
  We have updated this paragraph to include that the values of the shear exponent and veer were calculated with a power-law fit of the wind speed and a linear fit of the wind direction, respectively.
- Figure 1, bottom left: radial ticks on the wind speed rose are probably mislabeled.
  We have updated this figure so that the radial ticks are labeled by percentages instead of frequency counts (see Figure 8 in this document). Note, the data was not mislabeled. The concentric rings on a wind rose (the radial ticks) are simply the frequency scale that the wind fell into each directional bin and are a function of the number of bins used to plot the histogram data. If you take every directional bin's frequency and add them up, you will get 1 or 100%.
- Table 1: Why do the percentages not add to 100 in the final column or across all combinations of WS/TI conditions?
  The reason for this is already included in the table caption: "The combined sum over a row does not add to 100% because of the filtering of some cases with poor power-law fits."
- Line 228: Typo - σ_{y,z_0} should probably be σ_{y_0,z_0}.
  This typo has been updated, thank you.
- Some references (e.g., Cheung et al. WES (2024a)) have an out-of-date citation (should be: Cheung, L., Yalla, G., Mohan, P., Hsieh, A., Brown, K., deVelder, N., Houck, D., Henry de Frahan, M. T., Day, M., and Sprague, M.: Modeling the effects of active wake mixing on wake behavior through large-scale coherent structures, Wind Energ. Sci., 10, 1403–1420, https://doi.org/10.5194/wes-10-1403-2025, 2025). Please double-check all references.
  Thank you for catching that. We have updated the reference accordingly and will also work with the journal's typesetting team to ensure that all references are properly formatted in the final proofs.

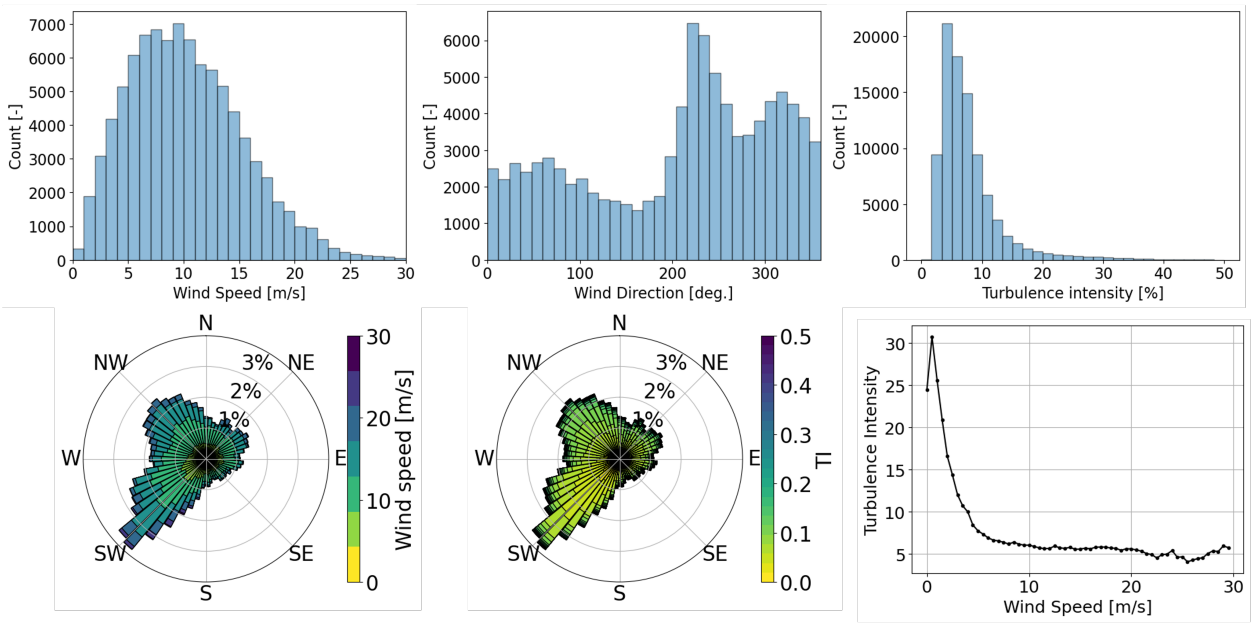

Figure 8: (Top) Histograms of wind speed, turbulence intensity, and wind direction at Site E06 in the NY Bight. (Bottom) Roses for wind speed and turbulence intensity, as well as turbulence intensity as a function of wind speed.

References

Frederik Aerts, Koen Devesse, and Johan Meyers. Bayesian uncertainty quantification of engineering models for wind-farm atmosphere interaction. Wind Energy Science Discussions, 2025:1–32, 2025.